Cabled marine magnetotellurics: denser data at lower cost and higher information content

Gary Egbert, Oregon State University; Naser Meqbel, GFZ Potsdam; Kurt Strack, KMS Technologies*

Summary

With the increasing success of marine electromagnetics, the trend is to go to similar acquisition density as with seismic data. Cabled marine controlled source electromagnetic (CSEM) systems under development will make acquisition of dense CSEM datasets for seafloor exploration practical. Natural source EM data, which may also be collected by such systems for essentially no additional cost, have the potential to refine and confine the interpretation of the CSEM data in complex and variable geologic environments. However, to reduce costs and maintain operational efficiency in a cabled system only some components of the EM fields may be collected, so that the configuration of sampled data may be non-standard for classical magnetotellurics. Specifically, spacings will be closer but not all components are measured at every site. Here we use 3D synthetic data inversion experiments to explore impacts on target recovery of (1) sampling density, and (2) exclusion of specific transfer function components. We show that including magnetic field TFs almost completely compensates for exclusion of impedance components associated with cross-profile electric fields, which would be more challenging to collect with a cabled system.

Introduction

While seismic offers the best description of reservoir shape and stratigraphy, it falls short in describing fluid and pore space properties. Usually, fluid discrimination with seismic waves depends on amplitude analysis, requiring true-amplitude migration of high-quality seismic data, something that is not always obtainable at reasonable cost. Electrical conductivity on the other hand responds directly to fluid properties (Schön, 2004), making electromagnetic methods a potentially valuable adjunct to seismic. Once the response of thin resistors to poloidal currents became widely understood (Eadie, 1979; Passalacqua, 1983), marine Controlled Source ElectroMagnetics (CSEM) methods developed rapidly (e.g., Cox, 1981; Cox et al., 1986; Sinha et al., 1990; Edwards and Yu, 1993; Constable and Cox, 1996, Eidesmo et al. 2002; Ziolkowski et al., 2006 and Constable, 2006) to the point where marine CSEM become a stable technology, commonly used in addition to 3D seismic for hydrocarbon exploration offshore.

All CSEM techniques are limited to the volume that is penetrated by the source, and to targets that produce sufficiently large responses at the receiver. For frequency domain EM the required source to receiver separation is several times the depth of investigation, such that 3D effects (caused by geologic variations between source and receiver) can seriously complicate interpretation. Smaller source-receiver offsets are possible with time domain EM, but in this case the anomalous response is smaller in deep water, and the key anomalous response occurs at long (tens of second) delay times. Vertical signal averaging is thus limited, as the source is moving. Natural source marine magnetotelluric (MT) data, which can be collected essentially for free once CSEM receivers are deployed, can be integrated with the CSEM measurements to overcome some of these challenges, e.g. by improving constraints on geological complexity surrounding exploration targets.

One of the biggest strengths of the seismic method is data redundancy. For marine CSEM data acquisition strategies that enable sampling densities that are “high enough” but still economically practical are required. Here we focus on this issue from the perspective of the MT data that might be acquired by a cabled seafloor data acquisition system, for which there may be many simultaneous receivers, but in a non-standard configuration for MT, with some components omitted to reduce cost. We explore the impact of sensor spacing, and omission of various transfer function (TF) components by inverting synthetic datasets generated for a suite of simple benchmark models.

ModEM Inversion

For inversion of the synthetic MT data we used ModEM, a modular (finite difference) 3D EM inversion code developed at Oregon State University (Egbert and Kelbert, 2012). To allow for experimentation with the full range of TFs that might be available with modern high-density cabled system, we implemented several new features in ModEM, adding capabilities for inclusion of horizontal magnetic inter-site TFs, and allowing the actual sampling configuration of the observing system to be represented more precisely (i.e., computing electric potentials between the actual electrode positions, and accounting for possible relative offsets of electric and magnetic sensors).

DOI http://dx.doi.org/10.1190/segam2013-1235.1

Synthetic Model Examples

Resistive features that are thin relative to depth of burial in the host produce very weak responses for MT sources, so our synthetic MT data tests focused on thicker resistive targets, representative of a "background geologic" feature such as a salt-dome (e.g., Comer and Newman, 2010). As specific examples here we consider two 50 ohm-m cubic targets buried 500 m below the sea floor in a water depth of 100 m. In the first case target (Figure 1) has dimensions of 4 x 4 x 3.6 km in X, Y and Z directions, respectively; for the second a smaller (2 x 2 x 2 km) resistive target is modeled. In both cases data are sampled in the period range 0.01-1000 s. Our primary objectives are to explore impacts on target recovery of (1) sampling density, and (2) exclusion of specific transfer function components. We initially considered E-W oriented profiles 500 m apart, with

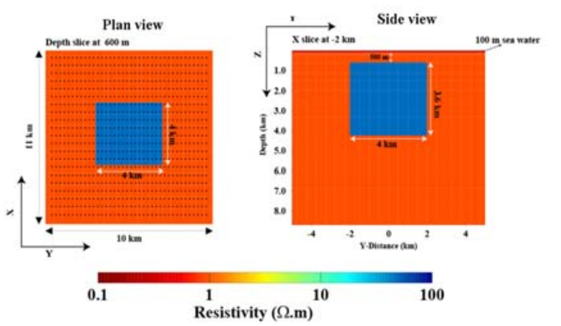

Figure 1: Benchmark model (large block) used for synthetic data inversion tests. Dots on plan view indicate nominal sampling locations for MT sites, at the finest sampling used (500 m between profiles, 250 m along profile).

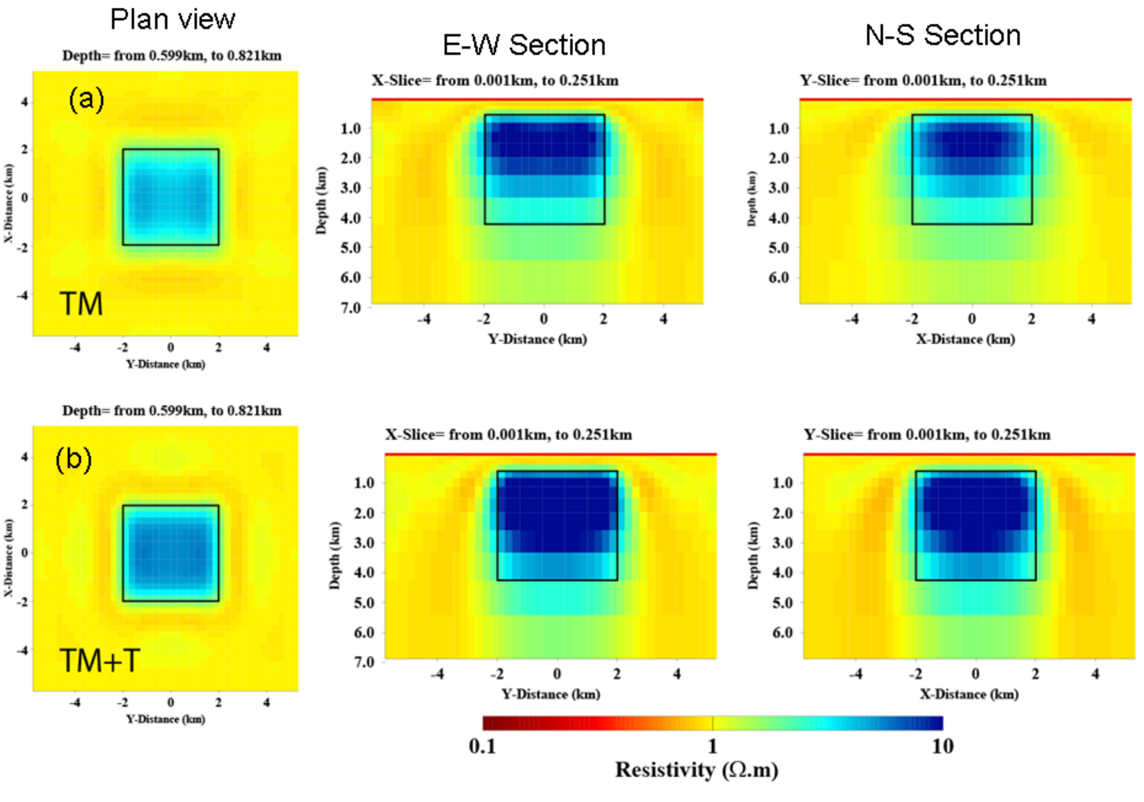

Figure2: 3-D inversion results for the larger target, showing plan and section views. (a) Results obtained with E_x component omitted (TM), b) Joint inversion of TM and T components results in very similar image quality as the full set of components (not shown). Sensors are 250m apart along profile, 500 m between profiles.

DOI http://dx.doi.org/10.1190/segam2013-1235.1

sensors spaced 250 m along profile, and then increased sensor spacing, both between and along profiles. The full dataset considered included all components of the MT impedance tensor (denoted **Z**), the vertical magnetic field TFs (**T**) and magnetic inter-station transfer functions (**M**). Then, specific components were excluded from the inversion in several combinations. In particular, we considered the case where the cross-profile component of the electric field might be omitted to reduce data acquisition costs. We refer to the remaining (along-profile) impedance component as "TM" in the following discussion.

Balancing fits to the different data types used in the inversion was often a challenge. The best results with our non-linear conjugate gradients search algorithm were obtained if we first fit the data that contains the most information about the resistivity of the target, namely, the **Z** components. **T,** and then **M,** components were then added successively and the expanded dataset was jointly inverted, starting from the previous inversion results.

Results

Representative examples of inversion results are shown in Figure 2 (large buried resistor) and Figure 3 (smaller target). The best results are of course obtained using all components, and the highest sampling density. In this case the outline of the target is recovered quite well, but the resistivity of the body is reduced to 20 ohm-m (from 50 ohm-m for the synthetic). For the TM only inversion (i.e., with E_x omitted) resolution of edges is poorer in the N-S direction, and the target resistivity is more severely underestimated (Fig. 2a). Adding **T** components (Figure 2b) improves results significantly, achieving nearly the same image quality as inversion of the full dataset. Further

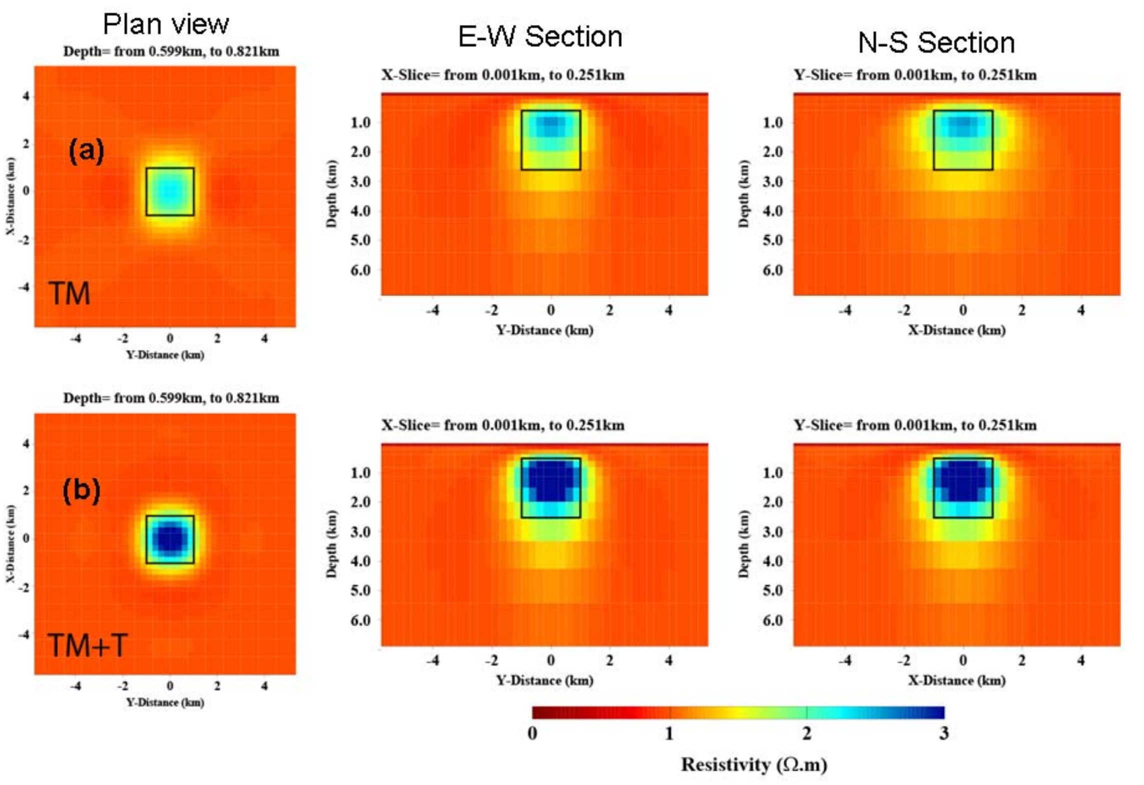

Figure 3: 3-D inversion results for the smaller resistive target. Note linear color scale—resistivity contrast is greatly reduced compared to Figure 1. a) Fitted data: only impedance tensor Z, with Ex components omitted (TM), b) joint inversion of TM and T components. Sensor spacing is identical to that of example of Fig. 1.

addition of the inter-station TFs **M** results in little further improvement in this case.

Turning to effects of sampling density, for this relatively large target very similar results (not shown) are obtained with sensor spacing doubled to 500 m along profile, and 1000 m between profiles. With even more widely spaced sensors image resolution degrades, and amplitudes drop to even lower levels. For the smaller target even at the highest sampling density with all TF components included the estimated resistivity contrast is severely attenuated (only 4 ohm-m), although target geometry is still reasonably recovered. Omitting E_x results in a further substantial reduction in amplitude, with peak amplitude just over 2 ohm-m (Figure 3a). Again, including **T** with the TM impedance data restores the image to nearly the same quality as obtained with the full dataset (Figure 3b).

Conclusions

One important conclusion that may be drawn from these tests is that including vertical magnetic field TFs (**T**) almost completely compensates for exclusion of the E_x impedance components. A second tentative conclusion is that the finest sampling considered (which other tests suggest would be optimal for controlled source applications) may be unnecessary for the MT. However the relatively simple examples considered so far raise questions which deserve further exploration. For example, we found that doubling sensor spacing (from 250 m along, 500 m between profiles) did not significantly degrade resolution of the spatial extent of the resistive target, and only slightly reduced contrasts. However, this result may well reflect specifics of the test case, with a homogeneous background, and a target burial depth of 500 m. Similar inversion tests should be conducted with more complex targets and background variations. With vertical field TFs (**T**) included there seemed to be little value in including also horizontal field TFs **M**. Further tests are warranted here also. E.g., we did not explicitly test if along profile variations of **M** might also compensate for the missing cross-profile electric field component (E_x). And, in situations with more complex targets, and more variable background variations, multiple TF components might well be expected to be more complementary than in the relatively simple test cases considered so far in this study.

Acknowledgments

The authors like to thank all the individuals who directly and indirectly supported this work. In particular, Tilman Hanstein helped with the OSU 3-D modeling/inversion project. We thank KMS Technologies for funding this work and the permission to publish http://dx.doi.org/10.1190/segam2013-1235.1

EDITED REFERENCES

Note: This reference list is a copy-edited version of the reference list submitted by the author. Reference lists for the 2013 SEG Technical Program Expanded Abstracts have been copy edited so that references provided with the online metadata for each paper will achieve a high degree of linking to cited sources that appear on the Web.

REFERENCES

Commer, M., and G. A. Newman, 2008, New advances in three-dimensional controlled-source electromagnetic inversion: Geophysical Journal International, **172**, no. 2, 513–535, http://dx.doi.org/10.1111/j.1365-246X.2007.03663.x.

Constable, S., 2006, Marine electromagnetic methods—A new tool for offshore exploration: The Leading Edge, **25**, 438–444, http://dx.doi.org/10.1190/1.2193225.

Constable, S., and C. S. Cox, 1996, Marine controlled source electromagnetic sounding 2: The PEGASUS experiment: Journal of Geophysical Research, **101**, B3, 5519–5530, http://dx.doi.org/10.1029/95JB03738.

Cox, C. S., 1981, On the electrical conductivity of the oceanic lithosphere: Physics of the Earth and Planetary Interiors, **25**, no. 3, 196–201, http://dx.doi.org/10.1016/0031-9201(81)90061-3.

Cox, C. S., S. C. Constable, A. D. Chave, and S. C. Webb, 1986, Controlled-source electromagnetic sounding of the oceanic lithosphere: Nature, **320**, no. 6057, 52–54, http://dx.doi.org/10.1038/320052a0.

Eadie, T., 1979, Stratified earth interpretation using standard horizontal loop electromagnetic data: Research in Applied Geophysics, no. 9, Geophysics Laboratory, Univ. of Toronto.

Egbert, G., and A. Kelbert, 2012, Computational recipes for electromagnetic inverse problems: Geophysical Journal International, **189**, no. 1, 251–267, http://dx.doi.org/10.1111/j.1365-246X.2011.05347.x.

Eidesmo, T., S. Ellingsrud, L. M. MacGregor, S. Constable, M.C. Sinha, S. Johansen, F. N. Kong, and H. Westerdahl, 2002, Sea bed logging (SBL), a new method for remote and direct identification of hydrocarbon filled layers in deep water areas: First Break, **20**, 144–152.

Passalacqua, H., 1983, Electromagnetic fields due to a thin resistive layer: Geophysical Prospecting, **31**, no. 6, 945–976, http://dx.doi.org/10.1111/j.1365-2478.1983.tb01099.x.

Schön, J. H., 2004, 1996, Physical properties of rocks: Fundamentals and principles of petrophysics: *in* Helbig, K. and S. Treitel, eds., Handbook of geophysical exploration - seismic exploration: 18 Pergamon Press (second edition 2004).

Sinha, M. C., P. D. Patel, M. J. Unsworth, T. R. E. Owen, and M. G. R. MacCormack, 1990, An active source electromagnetic sounding system for marine use: Marine Geophysical Researches, **12**, no. 1-2, 59–68, http://dx.doi.org/10.1007/BF00310563.

Webb, S., R. N. Edwards, and L. Yu, 1993, First measurements from a deep-tow transient electromagnetic sounding system: Marine Geophysical Researches, **15**, no. 1, 13–26, http://dx.doi.org/10.1007/BF01204149.

Ziolkowski, A., G., Hall, D. Wright, R. Carson, O. Peppe, D. Tooth, J. Mackay, and P. Chorley, 2006, Shallow marine test of MTEM method: 76th Annual International Meeting, SEG, Expanded Abstracts, 729–734.

DOI http://dx.doi.org/10.1190/segam2013-1235.1